Materials Physics and Mechanics. 2023;51(4): 66-75
Research article
http://dx.doi.org/10.18149/MPM.5142023_6

Submitted: May 11, 2023
Approved: June 9, 2023
Accepted: July 6, 2023

Peculiarities of the two-stage Zn diffusion profile formation from vapor phase into InGaAs/InP heterostructure for avalanche photodiode fabrication

S.A. Blokhin [1] ✉, R.V. Levin [1], V.S. Epoletov [1], A.G. Kuzmenkov [1], A.A. Blokhin [1], M.A. Bobrov [1], Ya.N. Kovach [1], N.A. Maleev [1], E.V. Nikitina [2], V.V. Andryushkin [3], A.P. Vasiljev [4], K.O. Voropaev [5], V.M. Ustinov [4]

[1] Ioffe Institute, St. Petersburg, Russia
[2] Alferov University, St. Petersburg, Russia
[3] Connector Optics LLC, St. Petersburg, Russia
[4] Submicron Heterostructures for Microelectronics, Research & Engineering Center, RAS, St. Petersburg, Russia
[5] JSC OKB-Planeta, Veliky Novgorod, Russia
✉ blokh@mail.ioffe.ru

Abstract. In this paper was presented the research results of the dependence of the InGaAs surface layer thickness on the process of Zn diffusion into InGaAs/InP heterostructures from a diethylzink source. One-dimensional distribution profiles of electrically active dopants were obtained by electrochemical volt-capacitive profiling. The influence of technological parameters (process time, temperature, and pressure in the reactor) on the hole concentration and the depth of the p-type dopant was studied. The principal possibility of simultaneously forming a highly doped InGaAs:Zn layer has been experimentally shown due to the higher Zn solubility limit in InGaAs compared to InP and to implement a two-stage p-type dopant profile in one Zn diffusion process by controlling the thickness of the InGaAs surface layer.
Keywords: zinc diffusion; diethylzinc; indium phosphide

Acknowledgements*. Authors thank RZD for financial support of the fabrication of InGaAs/InP heterostructures for comprehensive studies of the Zn diffusion process.*

Citation: Blokhin SA, Levin RV, Epoletov VS, Kuzmenkov AG, Blokhin AA, Bobrov MA, Kovach YN, Maleev NA, Nikitina EV, Andryushkin VV, Vasiljev AP, Voropaev KO, Ustinov VM. Peculiarities of the two-stage Zn diffusion profile formation from vapor phase into InGaAs/InP heterostructure for avalanche photodiode fabrication. *Materials Physics and Mechanics.* 2023;51(4): 66-75. DOI: 10.18149/MPM.5142023_6.

© S.A. Blokhin, R.V. Levin, V.S. Epoletov, A.G. Kuzmenkov, A.A. Blokhin, M.A. Bobrov, Ya.N. Kovach, N.A. Maleev, E.V. Nikitina, V.V. Andryushkin, A.P. Vasiljev, K.O. Voropaev, V.M. Ustinov, 2023.
Publisher: Peter the Great St. Petersburg Polytechnic University
This is an open access article under the CC BY-NC 4.0 license (https://creativecommons.org/li-censes/by-nc/4.0/)

Introduction

The most promising approach for the creation of compact telecommunication range single photon detectors is the usage of avalanche photodiodes (APDs) with a planar design based on InP-InGaAs heterostructures, where the photon absorption region in the InGaAs layer and multiplication of the photogenerated charge carrier region in the InP layer are separated [1,2]. The key point in the manufacturing of this type of APD is the formation of a two-stage p-type doping profile in the InP layer. For these purposes, a local Zn diffusion process into the InP layer through a dielectric mask [3,4] is used based on one of several technological approaches: Zn diffusion from a coated Zn_3P_2 or Zn_3P_2/Zn layer [5,6], diffusion in a sealed ampoule using a planar source based on Zn_3P_2 [7,8], Zn diffusion through a narrow gap using a planar source based on Zn_3P_2 [9,10], diffusion from the vapor phase in an open tube [4,11].

One of the main problems of the mentioned above approaches is the low level of p-type dopant concentration in the InP layer, which makes it difficult to form high-quality ohmic contacts to the p-InP layers. The simplest solution is the use of Zn-containing metal contacts [4,10]. However, the usage of Zn-containing metal contacts is associated with several new problems, such as low reliability, complex surface morphology and deep penetration of contact metallization materials into the p-InP layer during contact annealing, which significantly affects the final characteristics of the device.

Another problem in the creation of effective single photon APDs is related to the formation of a two-stage p-type dopant profile with local diffusion of Zn, which is necessary to suppress the local edge electric breakdown in the single photon APD [12,13]. There are two main approaches. The first one is based on double Zn diffusion processes through two different dielectric masks [11,14] and requires high reproducibility of the process and uniformity of the Zn diffusion over the sample area. The implementation of this approach is potentially possible from the vapor phase using metal-organic chemical vapor deposition (MOCVD) reactors [15,16]. The second approach is based on the formation of the InP layer surface relief followed by a single Zn diffusion process through dielectric mask [4,5,10] and requires the formation of a flat bottom of the etching well with smooth walls to suppress undesirable local electrical breakdown on the roughness of the Zn diffusion front. It is difficult to ensure a flat bottom of the well using non-selective chemical etching, and the use of stop layers for the implementation of a selective chemical etching is associated with a lateral anisotropic etching under the mask [17]. A plasma chemical etching of the InP layer potentially allows to provide the necessary parameters of the well [10], however, a few studies have noted its negative effect on the dark counts of the single photon APD [18].

A potential solution to these problems is the use of the InGaAs surface layer, which makes it possible to achieve a p-type doping level above 1×10^{19} cm^{-3} due to a higher Zn solubility limit in InGaAs compared to InP layers [19] and to apply the selective chemical etching through InAlAs/InGaAsP stop layers to form the required surface relief. A few studies have shown the possibility of Zn diffusion into InP layers from the vapor phase through the InGaAs layer [20-23] and demonstrated the usage of such technology for creating high-speed photodiodes in waveguide geometry [23]. The technological parameters of the Zn diffusion process from the vapor phase and type of Zn atom source set the concentration and the depth of the Zn diffusion into the InP layer [4,11,15,16,19,25,26]. However, the difference between the Zn solubility limits in the InP and InGaAs layers leads to some features of the Zn diffusion process into InP through the InGaAs layer [20-22].

This paper presents a study of the InGaAs surface layer thickness influence on the Zn diffusion process into the InP layer through the InGaAs layer from the diethylzinc (DEZn) metal organic source. The dependences of the obtained distribution profile of the electrically active p-type dopant on the process time, temperature, and pressure in the reactor during the technological process are considered.

Experiment

The investigated InGaAs/InP heterostructures were grown on the InP substrates and consisted of an undoped InP 3.5 μm thick layer, an undoped InGaAs 50 nm thick layer, an undoped InAlAs 10 nm thick stop layer and an undoped InGaAs 250 nm thick surface layer. The InGaAs surface layer thickness was varied by dry etching.

The process of Zn diffusion from the vapor phase into InGaAs/InP heterostructures was produced at the MOCVD Aixtron AIX-200 system. DEZn was used as a source of Zn atoms and hydrogen (H_2) was used as a carrier gas. The maximum flow of DEZn was ~$2.55 \cdot 10^{-5}$ mol/min at a thermostat temperature of 17°C. A stabilizing flow of arsine (AsH_3) was fed into the reactor to prevent surface degradation of the InGaAs layer at temperatures above 400 °C. The temperature range of the Zn diffusion process below 460 °C is limited by the precipitation of Zn compounds in the solid phase, and at temperatures above 550 °C the temperature range is limited by the deterioration of the surface morphology of the InGaAs layer. The amount of electrically active p-type dopant in the InP layer also depends on the parameters of the thermal activation dopant process [21,26,27]. After the Zn diffusion process, InGaAs/InP heterostructure samples were subjected to ex-situ rapid thermal annealing (RTA) in a nitrogen flow at 450 °C for 5 min.

The unidimensional distribution profiles of electrically active dopants in the studied InGaAs/InP heterostructures after Zn diffusion and RTA processes were determined by electrochemical capacitance-voltage profiling (ECV).

To carry out local diffusion into InP through a thin InGaAs layer a SiN_x dielectric mask with window topology was formed on the surface of InGaAs/InP heterostructures [28]. To obtain a two-stage profile of a p-type dopant in a single Zn diffusion process recesses with a defined shape and depth were etched within the dielectric mask windows (which defined the photosensitive region) formed on the surface of InGaAs/InP heterostructures. The recesses were made by selective chemical etching of the InGaAs layer to the InAlAs stop layer, followed by selective removal of the InAlAs stop layer.

Two-dimensional distribution profiles of electrically active p-type dopants in the studied samples were controlled by contrast on cross-sectional images obtained by scanning electron microscopy (SEM). SEM images were obtained in the secondary electron mode at low (<5 keV) accelerating voltages.

Results and discussion

Figure 1 shows the distribution profiles of electrically active p-type dopants in InGaAs/InP heterostructures depending on the thickness of the InGaAs surface layer, which demonstrates the effect of the InGaAs surface layer thickness on the Zn diffusion process. The process temperature was 500 °C, the reactor pressure was 50 mbar, and the process time was 60 minutes. In the direction from the surface of the structure the concentration of holes in the InGaAs layer monotonically decreases and its maximum value in the InGaAs layer reaches $(3–4) \cdot 10^{19}$ cm^{-3}, which is sufficient for the formation of ohmic contacts [19,24]. In this case, the near-surface region (~ 10-30 nm) is excluded from consideration because it is affected by the depletion of the surface and/or the effect of reverse diffusion near the surface. The local decrease in the hole concentration to $6 \cdot 10^{18}$ cm^{-3} coincides with the position of the InAlAs stop layer. The first sharp decrease in the hole concentration to $(1–3) \cdot 10^{18}$ cm^{-3} coincides with the position of the InGaAs-InP interface [21]. The second sharp drop below $1 \cdot 10^{17}$ cm^{-3} is related to the Zn diffusion front [29]. There is a sharp increase in the depth of the p-type dopants (at the level of $1 \cdot 10^{17}$ cm^{-3}) and an increase in the maximum concentration of holes in the InP layer to $3 \cdot 10^{18}$ cm^{-3} as the thickness of the InGaAs surface layer decreases. This is due to the existence of an initial transitional stage of Zn diffusion in the InGaAs/InP heterostructure when Zn diffusion first occurs only in the InGaAs layer. The demonstration of the hole segregation

effect in the InGaAs layer near the InGaAs-InP heterointerface is due to the higher limit of solubility of the Zn dopant in the InGaAs layer.

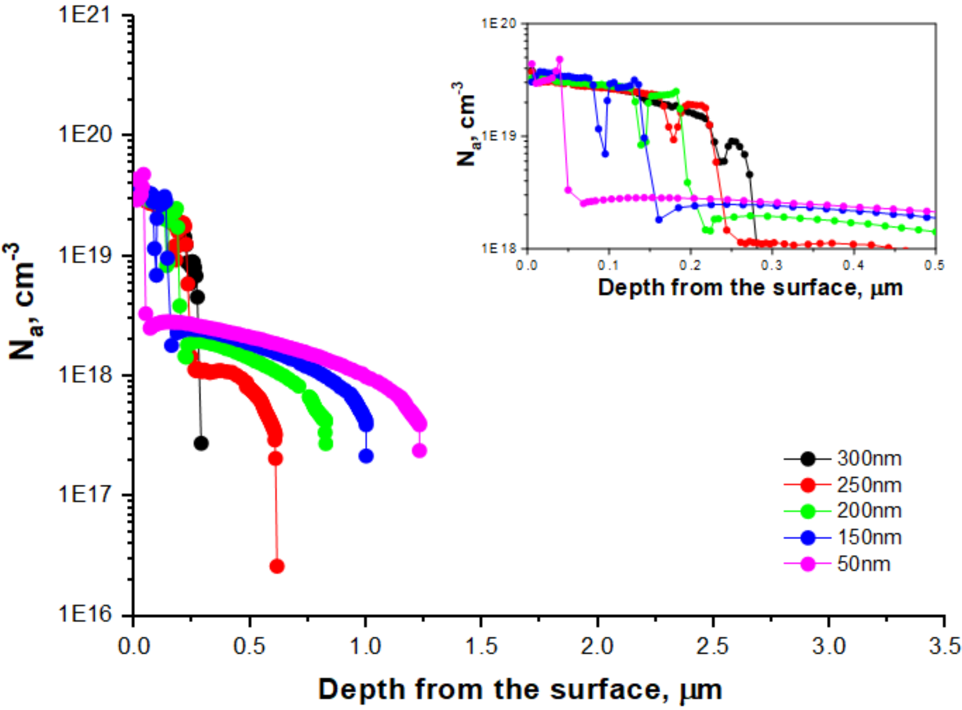

Fig. 1. Distribution profiles of electrically active p-dopants in the InGaAs/InP heterostructure for different thicknesses of InGaAs surface layer measured by ECV profiling. Temperature: 500 °C, pressure: 50 mbar, process time: 60 min

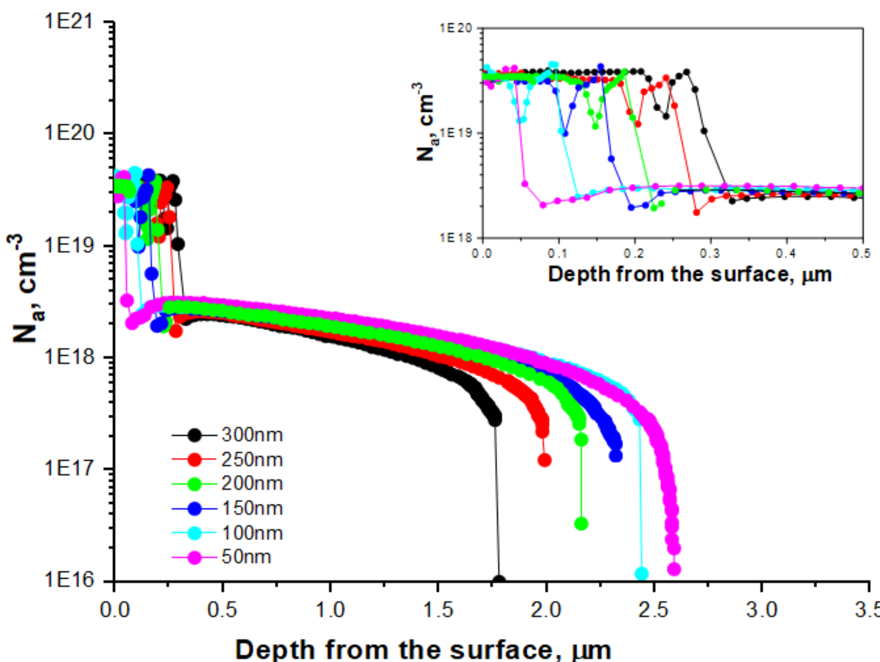

Fig. 2. Distribution profiles of electrically active p-dopants in the InGaAs/InP heterostructure for different thicknesses of InGaAs surface layer measured by ECV profiling. Temperature: 500 °C, pressure: 50 mbar, process time: 180 min

Figure 2 shows the distribution profiles of electrically active p-type dopants in InGaAs/InP heterostructures with different thicknesses of the InGaAs surface layer for a process time of 180 min with other fixed technological parameters. An increase in the Zn diffusion process time made it possible to achieve saturation of the hole concentration at the level of $(3–4)\cdot10^{19}$ cm^{-3} over the entire thickness of the InGaAs layer (with the exception of the InAlAs stop layer) and minimize the difference in the maximum hole concentration in the InP layer. Thus, Zn diffusion from an infinite solid-state source mode was realized (the concentration of the diffusant was constant). More detailed studies of the effect of the process time on the Zn diffusion in the InGaAs/InP have shown that in the case of saturation of the hole concentration in InGaAs, the difference in the depth of the Zn diffusion front in InP between samples with different thickness of the InGaAs surface layer remains constant.

An important issue is the influence of the Zn diffusion process temperature with the other fixed technological parameters. According to Fig. 3 a decrease in temperature from 500 to 475 °C leads to an increase in the maximum hole concentration in the InGaAs layer to $5.5\cdot10^{19}$ cm^{-3} and to an increase in the maximum hole concentration in the InP layer to $5.5\cdot10^{18}$ cm^{-3} and in the depth of the p-type dopant occurrence. This behavior is apparently due to an increase in the amount of diffusant due to a decrease in the desorption of Zn from the near-surface region with a decrease in the process temperature (similarly with the Zn diffusion into the InP layer [4,26] and into the InGaAs layer [19]). In addition, there is an increase in the effect of hole segregation in the InGaAs layer near the InGaAs-InP heterointerface and a sharp decrease in the difference of the Zn diffusion front depth in InP layer between samples with different thicknesses of the InGaAs surface layer, especially at thicknesses less than 200 nm. It should be noted that an increase in temperature during the Zn diffusion process leads to a drop of the near-surface diffusant concentration due to increased desorption and, as a result, to decreased hole concentration and depth of the Zn diffusion into the InP layer.

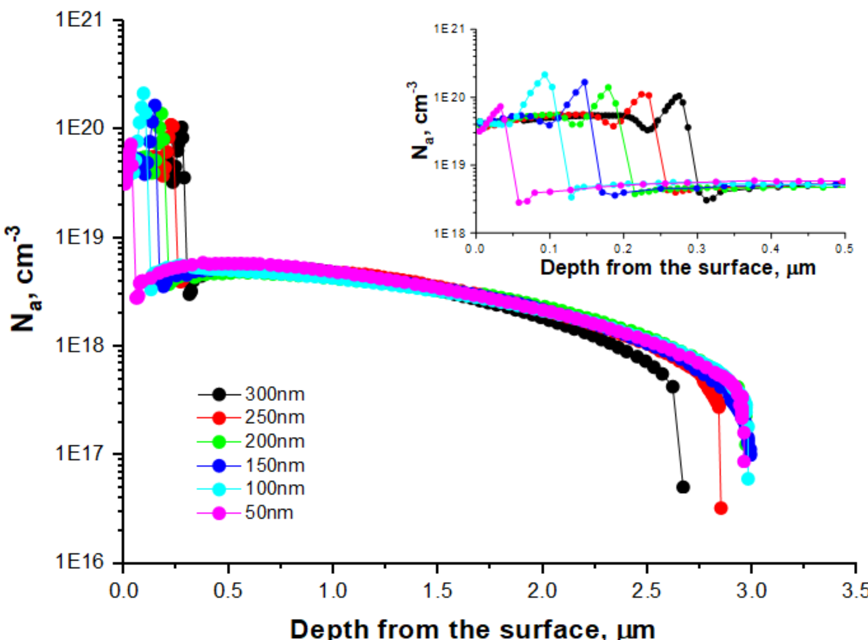

Fig. 3. Distribution profiles of electrically active p-dopants in the InGaAs/InP heterostructure for different thicknesses of InGaAs surface layer measured by ECV profiling. Temperature: 475 °C, pressure: 50 mbar, process time: 180 min

The effect of reactor pressure on Zn diffusion in InGaAs/InP was analyzed depending on the thickness of the InGaAs surface layer. The process temperature was 500 °C and the process time was 60 minutes. According to Figure 4 an increase in pressure in the reactor from 50 to 200 mbar leads to a sharp increase in the maximum hole concentration in the InGaAs layer to $8 \cdot 10^{19}$ cm^{-3}. Moreover, it leads to the disappearance of a local decrease of the hole concentration in the InAlAs stop layer and an increase in the effect of hole segregation near the InGaAs-InP heterointerface. The observed decrease of the hole concentration in the InGaAs layer near the surface is due to the process of reverse diffusion near the surface, for example, during sample cooling or thermal activation of a p-type dopant [4,21]. The high diffusant concentration in the InGaAs layer made it possible to reduce the depth spread and to obtain the Zn diffusion depth in the InP layer of more than 2.5 μm in a significantly shorter process time. At the same time, there is a sharp increase (compared with the results in Figs. 1 and 2) in the maximum hole concentration in the InP layer to $7 \cdot 10^{18}$ cm^{-3} which is comparable to the results of Zn diffusion from dimethylzinc into the InP layer [4,11,26]. This behavior is similar to the effect of the temperature decreasing and shows an increase in the diffusant concentration due to the suppression of Zn desorption from the near-surface region with an increase in pressure. At higher pressures in the reactor the solubility of the Zn dopants in the InGaAs layer is possibly limited, so the permeability of the InGaAs:Zn layer deteriorates, which negatively affects the Zn diffusion depth into the InP layer.

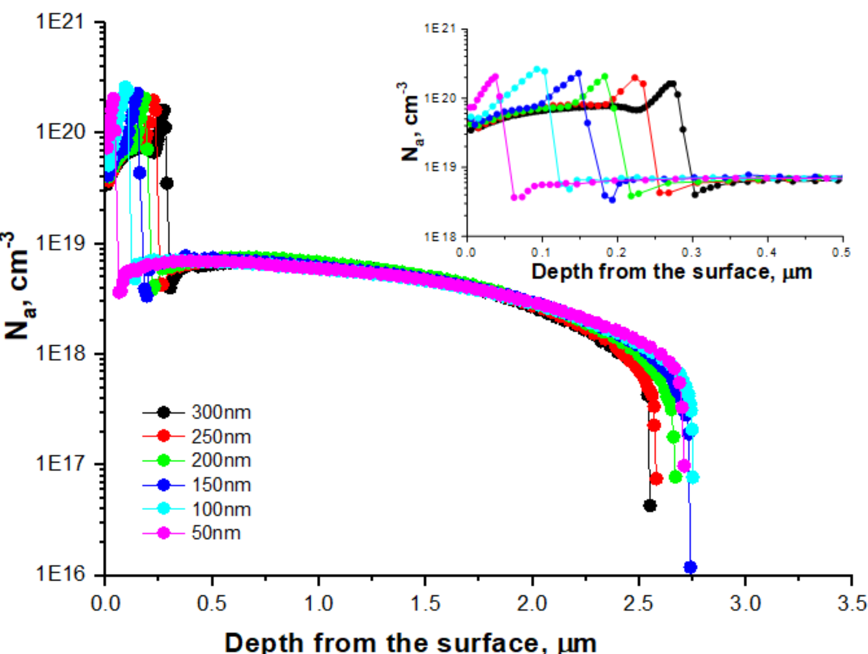

Fig. 4. Distribution profiles of electrically active p-dopants in the InGaAs/InP heterostructure for different thicknesses of InGaAs surface layer measured by ECV profiling. Temperature: 500 °C, pressure: 200 mbar, process time: 60 min

Thus, it can be concluded that during the Zn diffusion process from the vapor phase into the InP layer through the InGaAs layer the thickness variation of the InGaAs surface layer makes it possible to effectively control the Zn diffusion depth in the InP layer.

Figure 5 shows a typical scanning electron microscope (SEM) cross-section image of a sample with local Zn diffusion through a SiN_x dielectric mask. The Zn diffusion process temperature was 500 °C, the reactor pressure was 50 mbar, and the process time was 180 minutes. The position of the Zn diffusion front in the InP layer was determined by the image contrast boundary between regions with different types of conductivity. It should be noted that

it is difficult to determine the absolute value of the diffused Zn depth by the contrast since the observed contrast is complexly related to the distribution of the electric field on the studied sample cross-section. Nevertheless, the relative distance Δd_{Zn} between the first and second local Zn diffusion fronts can be estimated with relatively high accuracy (the measurement error does not exceed 10 %). At the etching depth Δd_{etch} of the InGaAs surface layer of about 0.2 μm the difference in the depth of the p-type dopant was 0.45 μm which is less than the target difference $\Delta d_{Zn} \sim 0.8$ μm, which was estimated from test processes of Zn diffusion into InGaAs/InP heterostructures without a dielectric mask. This effect can be caused both by an effective increase of the diffusant concentration in the near-surface region using a dielectric mask and by an inaccuracy of determining the depth of the p-type dopant in test processes by ECV profiling due to the curvature of the recesses bottom at large etching depths.

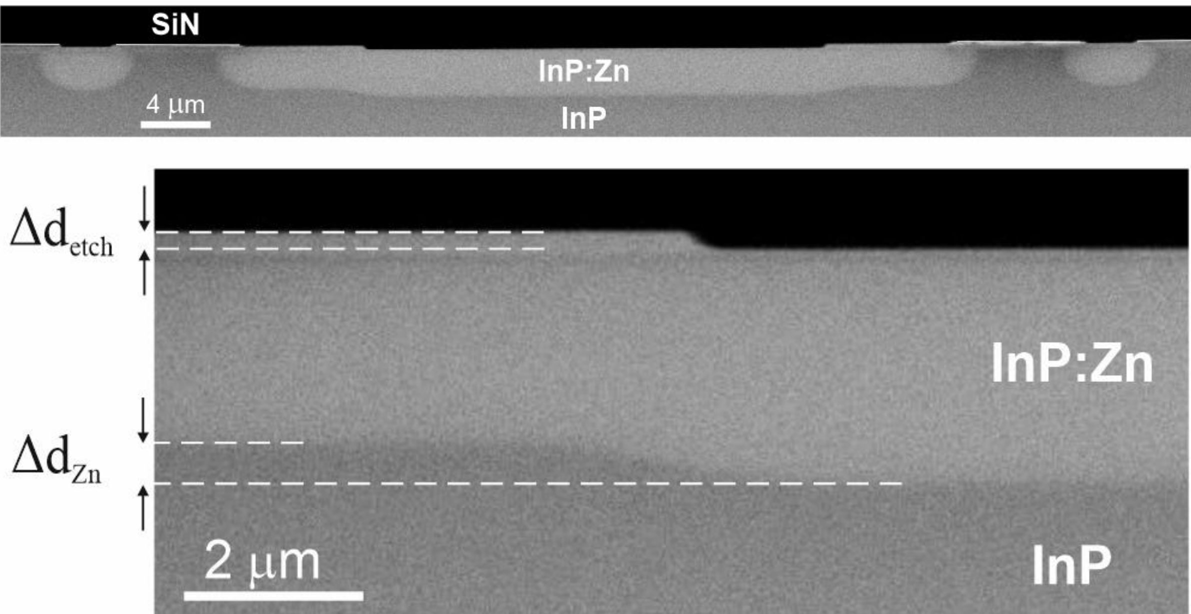

Fig. 5. SEM cross-section image of a sample with local diffusion of Zn into InGaAs/InP through a SiNx dielectric mask with a variation in the thickness of the InGaAs surface layer within the central window. Temperature 500 °C, pressure 50 mbar, process time 180 min

Conclusion

The results of the Zn diffusion from the vapor phase into the InP layer through the InGaAs surface layer with various thicknesses are presented. The Zn diffusion process was carried out according to the open tube scheme in the MOCVD reactor, where DEZn was used as a Zn source.

It was shown that a decrease of the InGaAs surface layer thickness leads to a sharp increase in the depth of the electrically active p-type dopant (Zn diffusion front at the level of $1 \cdot 10^{17}$ cm^{-3}). Additionally, an increase in the process temperature from 475 to 500 °C with other fixed technological parameters leads not only to a decrease of the hole concentration in the InGaAs surface layer and the depth of the p-type dopant but also to the increased difference in the depth of the Zn diffusion front with variations in the thickness of the InGaAs surface layer. An increase of the pressure in the reactor from 50 to 200 mbar with other fixed technological parameters leads to a sharp decrease in the difference of the Zn diffusion depth with variations in the thickness of the InGaAs surface layer.

The revealed behavior is due to the existence of an initial transitional stage of Zn diffusion into the InGaAs/InP heterostructure when Zn diffusion first occurs only in the InGaAs surface layer until the full saturation of the hole concentration is reached in it. At the same time, an

increase of the effective hole concentration in the InGaAs layer due to a weakening of the Zn desorption from the near-surface region (with a decrease in temperature and/or an increase in pressure in the reactor) leads to a faster implementation of the Zn diffusion process from an infinite solid-state source.

The studies have shown the principal possibility of controlled formation of a two-stage diffusion profile of a p-type dopant in a single Zn diffusion process from the vapor phase through the dielectric mask SiN_x into the InP layers by controlling the thickness of the InGaAs surface layer. This approach makes it possible to simultaneously provide a high level of p-type doping in the InGaAs surface layer, which is important for the formation of an ohmic p-contact. The results are important for the creation of single-photon APDs for quantum communication systems.

References

1. Zhang J, Itzler MA, Zbinden H, Pan JW. Advances in InGaAs/InP single-photon detector systems for quantum communication. *Light: Science & Applications*. 2015;4(5): e286–e286.
2. Ceccarelli F, Acconcia G, Gulinatti A, Ghioni M, Rech I, Osellame R. Recent Advances and Future Perspectives of Single-Photon Avalanche Diodes for Quantum Photonics Applications. *Advanced Quantum Technologies*. 2021;4(2): 2000102.
3. Tosi A, Calandri N, Sanzaro M, Acerbi F. Low-Noise, Low-Jitter, High Detection Efficiency InGaAs/InP Single-Photon Avalanche Diode. *IEEE Journal of selected topics in quantum electronics.* 2014;20(6): 192–197.
4. Jun DH, Jeong HY, Kim Y, Shin C-S, Park KH, Park W-K, Kim M-S, Kim S, Han SW Moon S. Single-step metal-organic vapor-phase diffusion for low-dark-current planar-type avalanche photodiodes. *Journal of the Korean Physical Society*. 2016;69(8): 1341–1346.
5. Kim MD, Baek JM, Kim TG, Kim SG, Chung KS. Characterization of double floating guard ring type InP-InGaAs avalanche photodiodes with Au/Zn low resistance ohmic contacts. *Thin Solid Films*. 2006;514(1–2): 250–253.
6. Chen Y, Zhang Z, Miao G, Jiang H, Song H. Optimized Selective-Area p-Type Diffusion for the Back-Illuminated Planar InGaAs/InP Avalanche Photodiodes by a Single Diffusion Process. *Physica Status Solidi (A)*. 2022;219(2): 2100577.
7. Lee K, Yang K. Analysis of InGaAs/InP Single-Photon Avalanche Diodes With the Multiplication Width Variation. *IEEE Photonics Technology Letters*. 2014;26(10): 999–1002.
8. Yun I, Hyun K-S. Zinc diffusion process investigation of InP-based test structures for high-speed avalanche photodiode fabrication. *Microelectronics Journal*. 2000;31(8): 635–639.
9. Preobrazhenskii VV, Chistokhin IB, Putyato MA, Valisheva NA, Emelyanov EA, Petrushkov MO, Pleshkov AS, Neizvestny IG, Ryabtsev II. Single Photon Detectors Based on InP/InGaAs/InP Avalanche Photodiodes. *Optoelectronics, Instrumentation and Data Processing*. 2021;57(5): 485–493.
10. Petrushkov MO, Putyato MA, Chistokhin IB, Semyagin BR, Emel'yanov EA, Esin MYu, Gavrilova TA, Vasev AV, Preobrazhenskii VV. Zinc Diffusion into InP via a Narrow Gap from a Planar Zn3P2-Based Source. *Technical Physics Letters*. 2018;44: 612–614.
11. Acerbi F, Tosi A, Zappa F. Growths and diffusions for InGaAs/InP single-photon avalanche diodes. *Sensors and Actuators A: Physical*. 2013;201: 207–213.
12. Jiang X, Itzler MA, Ben-Michael R, Slomkowski K. InGaAsP–InP Avalanche Photodiodes for Single Photon Detection. *IEEE Journal of Selected Topics in Quantum Electronics*. 2007;13(4): 895–905.
13. Signorelli F, Telesca F, Conca E, Della Frera A, Ruggeri A, Giudice A, Tosi A. Low-Noise InGaAs/InP Single-Photon Avalanche Diodes for Fiber-Based and Free-Space Applications. *IEEE Journal of Selected Topics in Quantum Electronics.* 2022;28(2): 1–10.

14. He T, Yang X, Tang Y, Wang R, Liu Y. High photon detection efficiency InGaAs/InP single photon avalanche diode at 250 K. *Journal of Semiconductors*. 2022;43(10): 102301.
15. Wada M, Seko M, Sakakibara K, Sekiguchi Y. Zn Diffusion into InP Using Dimethylzinc as a Zn Source. *Japanese Journal of Applied Physics.* 1989;28(10A): L1700.
16. Wisser J, Glade M, Schmidt HJ, Heime K. Zinc diffusion in InP using diethylzinc and phosphine. *Journal of Applied Physics.* 1992;71(7): 3234–3237.
17. Lee K, Lee B, Yoon S, Hong JH, Yang K. A Low Noise Planar-Type Avalanche Photodiode using a Single-Diffusion Process in Geiger-Mode Operation. *Japanese Journal of Applied Physics.* 2013;52(7R): 072201.
18. Lee K, Yang K. Performance comparison of wet-etched and dry-etched Geiger-mode avalanche photodiodes using a single diffusion process. *Physica Status Solidi (C)*. 2013;10(11): 1445–1447.
19. Franke D, Reier FW, Grote N. Post-growth Zn diffusion into InGaAs/InP in a LP-MOVPE reactor. *Journal of Crystal Growth*. 1998;195(1–4): 112–116.
20. Andryushkin VV, Gladyshev AG, Babichev AV, Kolodeznyi ES, Novikov II, Karachinsky LYa, Rochas SS, Maleev NA, Khvostikov VP, Ber BYa, Kuzmenkov AG, Kizhaev SS, Bougrov VE. Investigation of the zinc diffusion process into epitaxial layers of indium phosphide and indium-gallium arsenide grown by molecular beam epitaxy. *Journal of Optical Technology*. 2021;88(12): 87–92.
21. Van Geelen A, De Smet TMF, Van Dongen T, Van Gils WMEM. Zinc doping of InP by metal organic vapour phase diffusion (MOVPD). *Journal of Crystal Growth*. 1998;195(1–4): 79–84.
22. D'Agostino D, Carnicella G, Ciminelli C, Thijs P, Veldhoven PJ, Ambrosius H, Smit M. Low-loss passive waveguides in a generic InP foundry process via local diffusion of zinc. *Optics Express*. 2015;23(19): 25143.
23. Blokhin SA, Levin RV, Epoletov VS, Kuzmenkov AG, Blokhin AA, Bobrov MA, Kovach YN, Maleev NA, Andryushkin VV, Vasil'ev AP, Voropaev KO, Ustinov VM. Zn diffusion from vapor phase into InGaAs/InP heterostructure using diethylzinc as a p-dopant source. *Materials Physics and Mechanics*. 2023;51(3): 38–45.
24. Zhang L, La X, Zhu X, Guo J, Zhao L, Wang W, Liang S. High Speed Waveguide Uni-Traveling Carrier InGaAs/InP Photodiodes Fabricated By Zn Diffusion Doping. *IEEE Journal of Selected Topics in Quantum Electronics*. 2022;28(2): 1–6.
25. Vanhollebeke K, D'Hondt M, Moerman I, Van Daele P, Demeester P. Zn doping of InP, InAsP/InP, and InAsP/InGaAs heterostructures through metalorganic vapor phase diffusion (MOVPD). *Journal of Electronic Materials*. 2001;30(8): 951–959.
26. Pitts OJ, Benyon W, Goodchild D, SpringThorpe AJ. Multiwafer zinc diffusion in an OMVPE reactor. *Journal of Crystal Growth*. 2012;352(1): 249–252.
27. Van Gurp GJ, Van Dongen T, Fontijn GM, Jacobs JM, Tjaden DLA. Interstitial and substitutional Zn in InP and InGaAsP. *Journal of Applied Physics*. 1989;65(2): 553–560.
28. Zou WX, Vawter GA, Merz JL, Coldren LA. Behavior of SiNx films as masks for Zn diffusion. *Journal of Applied Physics*. 1987;62(3): 828–831.
29. Hampel CA, Blaauw C, Haysom JE, Glew R, Calder ID, Guillon S, Bryskiewicz T, Puetz N. Metalorganic vapor phase diffusion using DMZn Part II: Determination of the interstitial zinc charge state from secondary ion mass spectroscopy measurements using the Boltzmann–Matano technique. *Journal of Vacuum Science & Technology A*. 2004;22(3): 916.

THE AUTHORS

Blokhin S.A.
e-mail: blokh@mail.ioffe.ru

Levin R.V.
e-mail: Lev@vpegroup.ioffe.ru

Epoletov V.S.
e-mail: vadep@yandex.ru

Kuzmenkov A.G.
e-mail: kuzmenkov@mail.ioffe.ru

Blokhin A.A.
e-mail: Aleksey.Blokhin@mail.ioffe.ru

Bobrov M.A.
e-mail: bobrov.mikh@gmail.com

Kovach Ya.N.
e-mail: j-n-kovach@itmo.ru

Maleev N.A.
e-mail: maleev.beam@mail.ioffe.ru

Nikitina E.V.
e-mail: nikitina@mail.ru

Andryushkin V.V.
e-mail: vvandriushkin@itmo.ru

Vasiljev A.P.
e-mail: Vasiljev@mail.ioffe.ru

Voropaev K.O.
e-mail: kirill.voropaev@novsu.ru

Ustinov V.M.
e-mail: vmust@beam.ioffe.ru